

Assessment of the medial head of the gastrocnemius muscle in functional compression of the popliteal artery

Jayandiran Pillai, MBBCh, BSc, FCS, CVS, Lewis J. Levien, FCS (SA), PhD (Med), Mark Haagensen, MBBCh, FC Rad (DSA), Geoffrey Candy, PhD, Michelle DV Cluver, (BSc HONs), and Martin G. Veller, FCS (SA) *Johannesburg, South Africa*

Objective: Nonfunctional popliteal entrapment is due to embryologic maldevelopment within the popliteal fossa. Functional entrapment occurs in the apparent absence of an anatomic abnormality. Gastrocnemius hypertrophy has been associated with the latter. Both forms of entrapment may cause arterial injury and lower limb ischemia. This study assessed the attachment of the medial head of the gastrocnemius muscle in healthy occluders and healthy nonoccluders.

Methods: Provocative tests were used to identify 58 nonoccluders and 16 occluders. Ten subjects from each group underwent magnetic resonance imaging evaluation of the popliteal fossa. The medial head of the gastrocnemius muscle attachment was assessed in the supracondylar, pericondylar, and intercondylar areas.

Results: In the occluder group, significantly more muscle was attached towards the femoral midline (supracondylar), around the lateral border of the medial condyle (pericondylar), and within the intercondylar fossa.

Conclusion: The more extensive midline position of the medial head of the gastrocnemius in occluders is likely to be a normal embryological variation. Forceful contraction results in compression and occlusion of the adjacent popliteal artery. The clinical significance of these anatomic variations remains unclear. However, these new observations may provide insight for future analysis of the causes and natural history of functional compression and the potential progression to clinical entrapment. (J Vasc Surg 2008;48:1189-96.)

The classic syndrome of popliteal fossa entrapment is due to embryological anomalies between musculotendinous insertions within the popliteal fossa and neurovascular bundle. Functional entrapment occurs in the apparent absence of an anatomic abnormality.¹⁻³ This condition was first described in symptomatic military recruits and highly trained athletes^{4,5} in whom calf muscle hypertrophy was believed to be the cause of the entrapment mechanism. However, provocative tests that cause gastrocnemius contraction (forceful plantar flexion) may compress and laterally displace the popliteal artery in up to 50% of normal, untrained individuals.^{3,6}

Apparent compression of the popliteal artery at various sites within the popliteal fossa has been noted on magnetic resonance imaging (MRI) during provocative testing. These sites are between plantaris and the medial head of gastrocnemius muscle (MHGM), between plantaris and popliteus, at the soleal sling, and between the MHGM and the lateral femoral condyle.^{1,7} There is no clear explanation why compression occurs at these levels. It is possible, however, that these findings are due to the biased selection of muscular individuals⁸ or to MRI artefacts created by different degrees of muscle contraction. The natural history

and cause of functional entrapment therefore remains unknown.

The normal attachment of the MHGM is to the popliteal surface of the femur just above the medial condyle, extending above the epiphyseal line. We hypothesize that an unrecognized variation in the attachment of the MHGM may be the cause of functional entrapment or compression. The aim of this study was to compare the MRI-visualized attachment of the MHGM to the back of the medial femoral condyle in a group of healthy untrained subjects in whom the popliteal artery occludes on forceful plantar flexion (occluders) with a group of similar subjects where this does not happen (nonoccluders).

MATERIALS AND METHODS

The posterior tibial pulse of 50 men (mean age, 38.4) and 38 women (mean age, 37.9) recruited from the Johannesburg Hospital and three pharmaceutical companies were assessed with a Doppler probe at rest and with forceful plantar flexion. Only subjects aged between 21 and 50 years were included and we attempted to recruit normally active adult volunteers. The study was approved by the Ethics Committee from the University of the Witwatersrand, and all volunteers consented to participate in the study.

Subjects were excluded from the study if they were competing athletes, exercised more than three times per week, had a history of vascular disease or symptoms (claudication, rest pain, paraesthesia), had diabetes mellitus, or had undergone lower limb surgical procedures. Individuals with a body mass index of $>30 \text{ mg/kg}^2$ were excluded because technical difficulties were anticipated with obese

Division of Vascular Surgery, Department of Surgery, University of the Witwatersrand.

Competition of interest: none.

Reprint requests: Jayandiran Pillai, PO Box 21006, Helderkruijn, Johannesburg 1733, South Africa (e-mail: vascular@telkomsa.net).

0741-5214/\$34.00

Copyright © 2008 Published by Elsevier Inc. on behalf of The Society for Vascular Surgery.

doi:10.1016/j.jvs.2008.06.057

individuals, including ankle-brachial index (ABI) measurements and cuff size, visualization of popliteal fossae structures, and ability to adequately contract the gastrocnemius muscle in the prone and upright position. Those aged >50 were excluded due to the anticipated higher prevalence of subclinical popliteal vascular disease, hypertension, diabetes mellitus, and age-related loss of calf muscle bulk and tone. Owing to the conflicting data regarding the role of gastrocnemius hypertrophy on popliteal artery compression,^{1,3} we attempted to exclude individuals with any degree of calf muscle hypertrophy.

Resistance during forceful plantar flexion was provided by the examiner's hand or a folded broad sheet that was wrapped under the plantar surface of the foot. The subject grasped both ends of the looped sheet firmly, thus providing counteractive resistance.⁹ These maneuvers were repeated with varying degrees of plantar flexion. If the Doppler signals of both posterior tibial pulses disappeared or clearly diminished during forceful plantar flexion, we assumed that the gastrocnemius muscle was compressing the popliteal artery and classified these volunteers as having bilateral functional occlusion (occluders). If the Doppler signals of both posterior tibial pulses were still present after maximal plantar flexion, we assumed the gastrocnemius muscle was not compressing the popliteal artery and classified these volunteers as not having functional occlusion (nonoccluders). Of the 88 subjects screened, 14 were not allocated to either of these groups (8 demonstrated a unilateral decrease in pulse status, and in 6 the pedal pulse status during forceful plantar flexion could not be clearly defined). We identified 16 bilateral occluders and 58 bilateral nonoccluders (Table I).

An attempt was made to measure ABIs in all individuals at rest and at maximal plantar flexion. Unlike others,¹⁰ however, we found that ABI measurements were not reliable in determining the degree of popliteal artery compression during plantar flexion and this strategy was abandoned.

The first 10 subjects from the occluder and the nonoccluder groups were selected for ultrasound evaluation of their popliteal fossae at rest and with forceful plantar flexion to confirm or exclude arterial compression within the popliteal fossa. Arterial compression was confirmed when there was an immediate, complete disappearance of the velocity waveform (together with disappearance of the imaged artery) or a gradual increase in the velocity waveform (with simultaneous narrowing of the imaged artery) on forceful plantar flexion. Subjects were classified as nonoccluders if the velocity waveforms and the ultrasound appearance of the artery remained unchanged at the end of forceful plantar flexion. In two subjects from the occluder group, compression of the popliteal artery in the popliteal fossa could not be confidently seen on the ultrasound examination, and two further occluders were recruited from the original group of 16. Ten bilateral occluders and 10 bilateral nonoccluders were therefore identified, and bilateral popliteal fossa MRIs were performed in each individual. Cost constraints only allowed 20 MRI examinations to be per-

formed; therefore, 20 limbs in each group were evaluated by MRI.

Magnetic resonance imaging. Volunteers were scanned on a Phillips 1.5-Tesla Intera System (Eindhoven, The Netherlands). Both knees of each participant were scanned in a dedicated quadrature knee coil. After survey scans, an axial turbo T2-weighted sequence (repetition time [TR], 5076 milliseconds; echo time [TE], 100 milliseconds; flip angle, 90; turbo field (TF), 13; 4-mm slices \times 24 with 1-mm gap, and two acquisitions) was obtained (acquisition time [TA], 2:37 minutes) to exclude any pathologic conditions such as enlarged bursae or popliteal cysts. Subsequently, both a sagittal and coronal T1-weighted volume acquisition was prescribed using 1-mm over-contiguous slices (TR, 25 milliseconds; TE, 4.6 milliseconds; flip angle, 30; matrix 336 \times 512; 70 slices; field of view, 220 with a rectangular field of view of 60%; number of acquisition, 2; and TA, 4:23 minutes). The T1-weighted sequences were exported to a Phillips workstation (MX viewer). Triplanar interactive reconstruction was used to initially align the coronal and sagittal data sets, first to the posterior margins of the femoral condyles and then to the long axis of the femur in both the coronal and sagittal planes.

For each of the T1 three-dimensional data sets using triplanar interactive reconstruction, the crosshairs were placed on the most medial and superior point of the insertion of the medial head of the gastrocnemius. A hard copy was made of the three images generated (ie, coronal, axial, and sagittal views). A fourth image was created in the coronal plane by scrolling backwards until the crosshairs intercepted the center of the popliteal artery. The same procedure was performed for both axial and sagittal T1 data sets. One last coronal view was obtained from the coronal data set only by rotating the crosshairs in the sagittal plane to align with the popliteal artery in the coronal view below the point of intersection. A hard copy was also made of this image, producing one film of nine images for each knee that was used for further analysis.

The MHGM attachment was assessed in three regions on MRI (Fig 1):

- *Supracondylar attachment:* Superior attachment along the popliteal surface of the femur was measured as a ratio, using four 1-mm, axial cuts (labelled 1-4; 1 being furthest away from the medial condyle and 4 being at the superior part of the medial condyle). Ratios of the width of the MHGM (w) to the widest diameter of the femur (f) were calculated; f was constructed from the most lateral to the most medial point of the femur (Fig 2). The greater the ratio, the more extensive the attachment towards the midline.
- *Pericondylar attachment:* Attachment around the superior and lateral aspects of the medial condyle. Coronal scans were used to visualize attachment of the MHGM to the superior margin of the medial condyle. On the coronal scan, the medial condyle was divided into four quadrants. Each quadrant was assigned a 25% capability of MHGM attachment (Fig 3). The extent

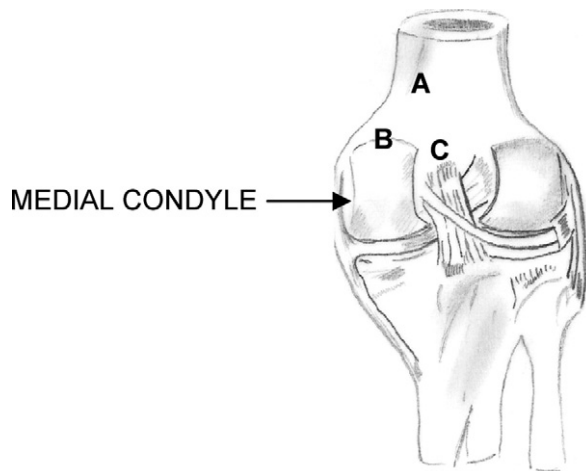


Fig 1. Posterior aspect of right femur. *A*, *B*, and *C* represent areas of attachment of the medial head of the gastrocnemius muscle that were examined by magnetic resonance imaging.

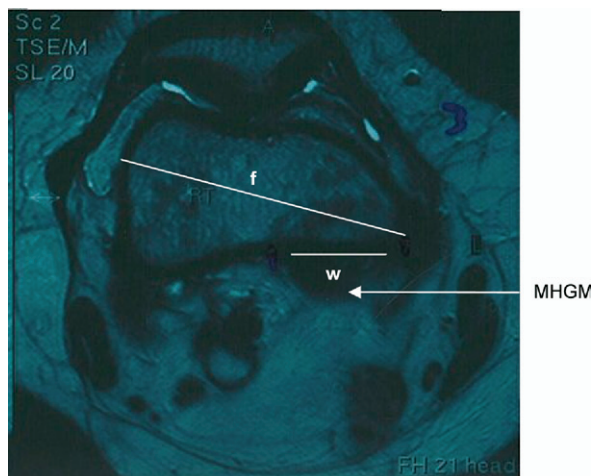


Fig 2. Axial scan of the distal right femur shows the attachment of the medial head of the gastrocnemius muscle (*MHGM*). Lines show the width of the femur (*f*) and the extent of lateral to medial (*w*) attachment of the *MHGM*.

of attachment was estimated as a percentage of circumferential attachment. A measuring protractor was used to calculate pericondylar attachment. The straight base of the protractor was placed on the midline (Fig 3).

- **Intercondylar attachment:** Attachment within the intercondylar notch. The intercondylar notch on an axial scan was divided into four equal segments. The extent of attachment of the *MHGM* within the notch was calculated as a sum of the segments to which the *MHGM* was attached (expressed as a percentage; Fig 4). A protractor was used to calculate intercondylar attachment.

All measurements were repeated by a radiologist who was blinded to the MRI groupings.

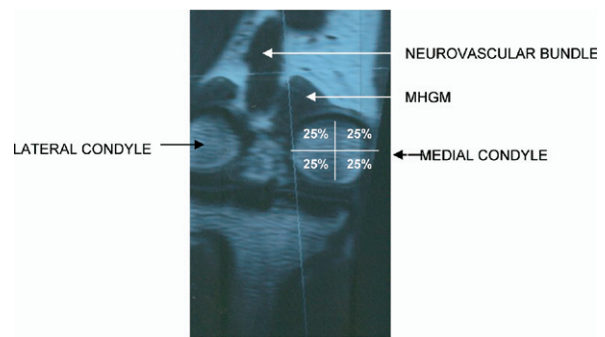


Fig 3. Coronal section of the right knee shows attachment of the medial head of the gastrocnemius muscle (*MHGM*) to the medial condyle. The *MHGM* is attached to 18% of the circumference of the medial condyle.

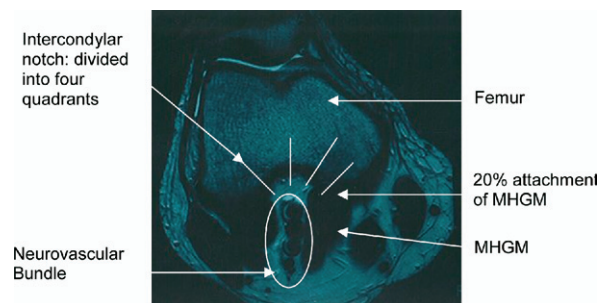


Fig 4. Axial scan of the right knee at the level of the intercondylar notch shows that 20% of the curve of the notch is occupied by medial head of the gastrocnemius muscle (*MHGM*) fibers.

We had initially intended to perform MRIs at rest and during forceful plantar flexion to identify compression of the neurovascular bundle. We found this technically difficult with the two strategies that we used (grasping a folded sheet and pushing against an examiner's hand). After 60 seconds of forceful plantar flexion, subjects found it difficult to maintain contraction and fatigue set in, which resulted in trembling and haphazard relaxation of plantar flexion. This significant movement occurred before the completed imaging period (>3 minutes). Images that were obtained appeared inadequate owing to movement-related artifact. There is possibly a learning curve to overcome before this technique can be standardized and reproduced.

Statistical analysis. Data are reported as frequency, and the mean and standard deviation (SD) was calculated. Differences between groups were determined using a *t* test for normally distributed data and a Kruskal-Wallis test for non-normally distributed data or when the sample size was small. A value of $P < .05$ was considered to be statistically significant.

RESULTS

Demographics. No statistical differences were found in age and weight between the screened (provocative test-

Table I. Demographics of the occluders and nonoccluders who underwent screening and magnetic resonance imaging evaluation

Variable	Nonoccluders		Occluders		P	
	Screened (n = 58)	MRI (n = 10)	Screened (n = 16)	MRI (n = 10)	Screened	MRI
Age, mean (SD), y	38.4 (9.55)	35.8 (5.04)	36.4 (10.30)	38.7 (10.42)	p = 0.47	p = 0.44
Sex, No.					.0137	.0286
Male	32	9	5	4		
Female	14	1	11	6		
Height, mean (SD), m	1.68 (0.10)	1.76 (0.12)	1.65 (0.12)	1.68 (0.05)	<.01	<.01
Weight, mean (SD), kg	71.11 (18.44)	78.29 (8.63)	70.85 (12.91)	73.86 (4.50)	p = 0.17	p = 0.44

MRI, Magnetic resonance imaging.

Table II. Supracondylar attachment: ratios of the medial head of the gastrocnemius muscle to the width of distal femur (20 limbs in each group)

Axial scans	Non-occluders, mean (range)	Occluders, mean (range)	P
1	0.39 (0.29-0.50)	0.40 (0.26-0.58)	.3
2	0.40 (0.32-0.50)	0.42 (0.32-0.55)	.1
3	0.42 (0.15-0.53)	0.48 (0.39-0.56)	.002
4	0.44 (0.34-0.51)	0.49 (0.36-0.60)	.009

ing and ultrasound popliteal fossa examination) 58 nonoccluders and 16 occluders or between the 10 nonoccluders and 10 occluders who underwent MRI examination (Table I). There were statistically more women in the screened and MRI-tested occluder group. There was a statistical difference in height. This discrepancy may be due to sampling error, and sex and height probably have little to do with popliteal occlusion.

Evaluation of MRIs. Analyses of the scans were not “blinded” to the authors who performed the initial measurements but were blinded to the independent radiologist. Although there were differences in actual measurements between the authors’ and radiologists’ data, both reported statistical significance in similar areas. Both parties reached consensus that none of the scans analyzed demonstrated any of the described forms of nonfunctional entrapment.

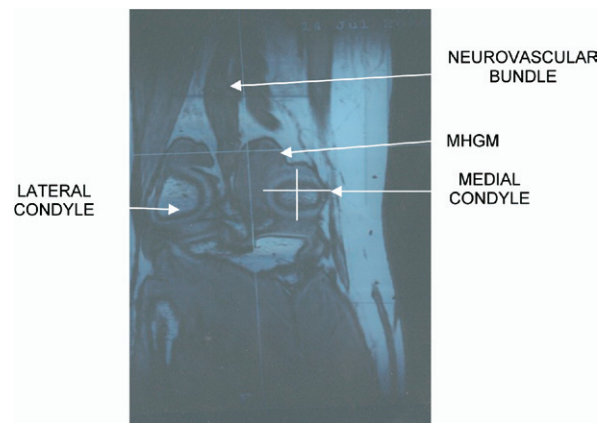
There was no difference in supracondylar ratios between the two groups in axial scans 1 and 2, which represent supracondylar attachment along the femur furthest away from the medial condyle ($P = .3$ and $P = 0.1$, respectively). The supracondylar attachment in scans 3 and 4, representing femoral attachment nearer the medial condyle, were statistically greater in the occluder group ($P = .002$ and $P = .009$, respectively; Table II). The latter indicates greater attachment of the muscle towards the midline of the femur in the occluder group.

The extent of the pericondylar and intercondylar attachment was significantly different between the two groups (Table III; Figs 5-10). The coronal pericondylar scans showed significantly more attachment of the MHGM fibers to the superior and lateral part of the medial condyle

Table III. Pericondylar and intercondylar attachment (20 limbs in each group)

MHGM attachment	Nonoccluders, mean % (range)	Occluders, mean % (range)	P
Pericondylar	22 (15-40)	38 (20-50)	<.001
Intercondylar	21 (15-40)	43 (25-70)	<.001

MHGM, Medial head of the gastrocnemius muscle.

**Fig 5.** Coronal scan of the right medial condyle in an occluder shows that 45% of the inner circumference of the medial condyle has medial head of the gastrocnemius muscle (MHGM) attached to it. The MHGM butts the neurovascular bundle within the intercondylar fossa.

in the occluder group ($P < .001$). Note in Fig 5 that the MHGM attaches to approximately 45% of the circumference of the medial condyle in an occluder and is close to the neurovascular bundle. In Fig 6 (nonoccluder), the MHGM is only attached to approximately 18% of the circumference of the medial condyle, and the anterior and posterior MHGM coronal scans did not reveal any further attachment of the MHGM fibers around the medial condyle such as depicted in Fig 5 (an occluder).

In 12 of the 20 MRIs in the occluders, a $\geq 40\%$ pericondylar attachment could be clearly seen to enter and fill the intercondylar notch on coronal scans. Only two of 20

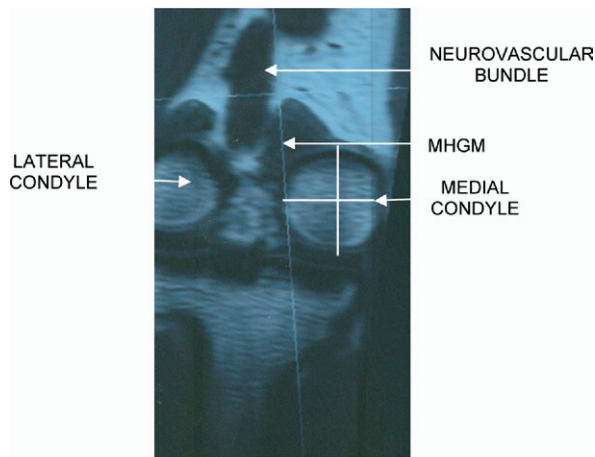


Fig 6. Coronal scan of the right medial condyle in a nonoccluder shows that 18% of the inner circumference of the medial condyle has medial head of the gastrocnemius muscle (MHGM) fiber attached. In none of the more posterior or anterior images do muscle fibers occupy a greater attachment around the circumference.

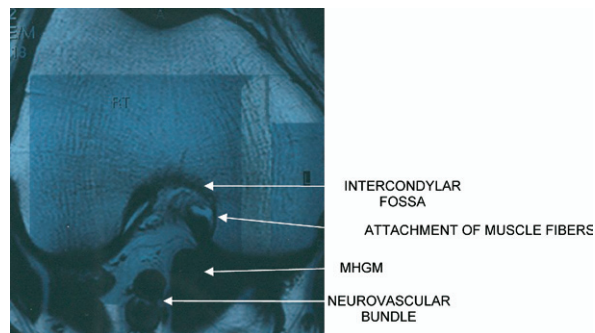


Fig 7. Axial scan of the right intercondylar notch in a nonoccluder shows 20% attachment of medial head of the gastrocnemius muscle (MHGM) fibers within the notch. The MHGM remains outside the fossa.

MRIs in the nonoccluder group revealed 35% and 40% pericondylar attachment, respectively.

On axial intercondylar scans there was significantly greater attachment of the MHGM within the notch in the occluder group ($P < .001$; Table III, Figs 7 and 8). Note in Fig 7 (nonoccluder) that the MHGM fibers sparsely enter the intercondylar fossa ($\pm 20\%$ attachment) and in none of the images obtained from this subject does muscle bulk fill the fossa. This is in comparison with an occluder (Fig 8), where 50% of the rim of the notch is attached by MHGM fibers that are close to the neurovascular bundle.

In 11 of 20 MRIs evaluated for intercondylar attachment in the occluder group, the MHGM was attached by $\geq 50\%$ to the rim of the fossa. In eight of these, bulky fibers of the MHGM were found to occupy considerable space within the fossa (Fig 8). None of the images in the nonoccluder group revealed a $>40\%$ attachment to the rim, nor

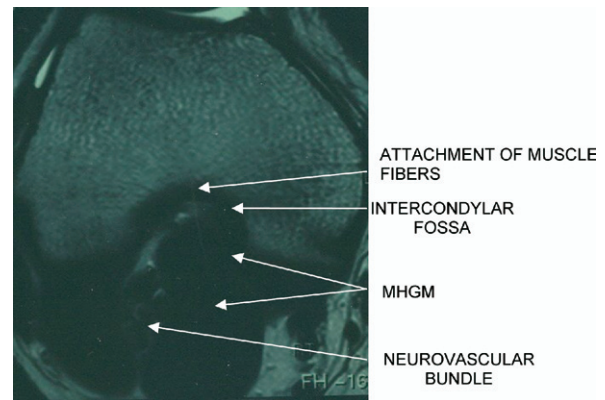


Fig 8. Axial scan of the right intercondylar notch in an occluder shows 50% attachment of medial head of the gastrocnemius muscle (MHGM) fibers within the notch. The MHGM is close to the neurovascular bundle and occupies greater space within the fossa.

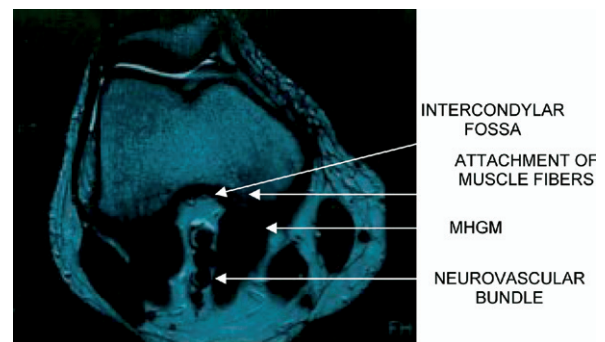


Fig 9. Axial scan of the right intercondylar notch in a nonoccluder shows 15% attachment of MHGM fibers within the notch.

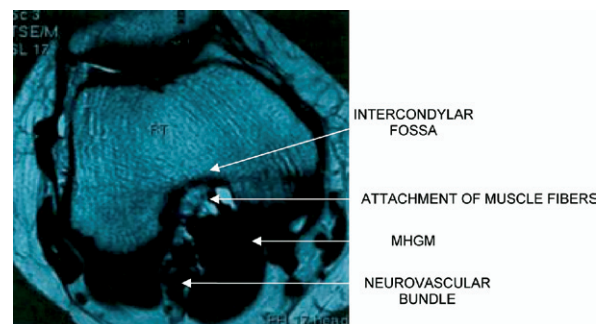


Fig 10. Axial scan of the right intercondylar notch in an occluder shows 70% attachment across the fossa.

did any reveal bulky MHGM fibers filling the fossa such as seen in Fig 8.

DISCUSSION

A review of the literature on functional popliteal entrapment reveals that the incidence of asymptomatic occlusion in the general population is 30% to 40% and ap-

proaches 50% in highly trained athletes.¹⁰ Hypertrophy of the MHGM has been implicated as a cause in highly trained athletes, although MRI studies suggest that arterial compression may occur at the level of the plantaris muscle above the knee and at the lateral edge of the soleal sling below the knee.¹ Symptoms are rare although the entity is common.¹ Endothelial damage and occlusion of the popliteal artery may occur in the presence of apparently normal fossa anatomy.¹¹

The cause, natural history, and precise incidence of functional entrapment therefore remain unclear. This study attempts to find a cause for functional popliteal artery compression within the popliteal fossa by assessing the MRI anatomy of the MHGM in normal volunteers.

Methods used. It was difficult to measure and interpret ABIs in the context of graded compression of the popliteal artery by the MHGM. For example, 30° of plantar flexion in a subject in whom the MHGM is bulky and fills the intercondylar fossa by 50% to 70% may result in a greater decrease of the ABI compared with a subject in whom the MHGM is less bulky near the midline. We found ABI measurements to be unreliable, however. The ABIs varied depending on the amount of force used to cause contraction, the size of the calf muscle, the size of the cuff used, and the position of the cuff in relation to muscle bulk. Extremely forceful contraction in some volunteers resulted in an increase in the ABI because higher pressure was needed to overcome the contracted calf muscle. Therefore, pressure measurements were not used to grade the volunteers.

We concede that screening of individuals (plantar flexion with Doppler ultrasound imaging of posterior tibial arteries and popliteal artery duplex assessment) has limitations and is subjective. When posterior tibial pulses during forceful plantar flexion are assessed, there is a change in the anatomic relationship between the artery and the adjacent muscle. This together with slight displacement of the transducer probe results in loss of signal and gives the impression of arterial occlusion. Two examiners repeated these maneuvers before volunteers were classified into one group or the other. To enhance the accuracy of screening, ultrasound examinations of the popliteal fossa were performed in occluders and nonoccluders.

Two patterns of occlusion seem to occur on sonographic assessment of the popliteal fossa. The first is an early and dramatic disappearance of the artery on plantar flexion as a result of movement of the gastrocnemius across the fossa. Realignment of the transducer may give the impression of a pulsating artery in a more lateral position. Changes in arterial velocity are inconsistent. The second is a gradual narrowing of the artery by the adjacent contracting gastrocnemius, with corresponding changes in the velocity, and compression of the artery is usually seen when plantar flexion is >60°. In the latter, lateral displacement of the artery may occur, but arterial compression can be followed until occlusion. Both of these forms were included in the occluder group and were not separately evaluated. Although the second appears to be a more accurate indication

of arterial compression by the contracting adjacent gastrocnemius muscle, there may be more than one occluding mechanism. To increase accuracy of both screening methods, measurements were repeated with realignment of the probe together with slow deliberate movement of the foot against resistance.

Although MRI clearly showed the anatomy of the popliteal fossa, we acknowledge that the interpretation of MRIs is relatively subjective. To minimize the risk of error and bias, bony and muscle measurements were performed using callipers and protractors. Bony landmarks were standardized. Measurements were repeated by an independent radiologist.

To limit intraobserver and interobserver variability, four different images were used to assess attachment of the same muscle around the medial condyle (2 supracondylar, 1 pericondylar, and 1 intracondylar). All four sets of results concur that in occluders, attachment of the MHGM is closer to the midline of the bone. On visual assessment of 12 images in the occluder group, MHGM fibers were clearly seen to occupy a more midline position (Figs 5 vs 6 and 7 vs 8). After discussions with the independent radiologist, we agreed that a significant number of images were very obviously different (occluders vs nonoccluders) and that further independent appraisal was not necessary. All measurements were performed at the bone-muscle interface, where strands of muscle fibers appeared to be attached to the bone. Errors related to measuring muscle bulk rather than attachment was thus avoided.

Embryology and classic entrapment syndrome.

The classic syndrome of popliteal fossa entrapment, which was recognized >100 years ago, is due to the anomalous relationship between musculotendinous insertions within the popliteal fossa and neurovascular structures.^{1,12} These anomalies begin during embryological development of the popliteal fossa, when the MHGM migrates across the fossa from lateral to medial and eventually attaches to the posterior surface of the medial femoral condyle.^{12,13}

The adult popliteal artery is divided into three embryological segments: proximal, middle, and distal.¹⁴ The proximal portion forms by fusion of the developing femoral and axial popliteal arteries. The middle portion is derived from a remnant of the axial artery. The distal portion forms superficial to the popliteus muscle by fusion of anterior and posterior tibial vessels.¹⁵ Migration of the MHGM from lateral to medial occurs at the same time as the three segments of the popliteal artery are fusing. Classic entrapment results when the popliteal artery develops more medially in relation to the MHGM, that is, types I and II.¹⁶ In embryological entrapment, which is type III, the entrapment mechanism is caused by fibrous and tendinous bands derived from remnants of the migrating medial head or mature muscle slips that displace and separate the neurovascular structures.¹⁷ As a result of the expansive embryological migration of the MHGM within a small space, it is possible that other as yet undescribed muscular anomalies exist.

Anatomic variation of the MHGM. Attachment of the MHGM to the femur just above the medial condyle, along the lateral part of the medial condyle, and extension into the intercondylar notch were significantly different in the two groups. There was more extensive attachment toward the midline of the bone just above the medial condyle as well as more extensive attachment of muscle fibers within the intercondylar notch in the occluder group (Figs 5-10). The corresponding muscle bulk occupying the intercondylar fossa was greater in the occluder group (Fig 8). As a result, it appears that there is a greater muscle bulk adjacent to the neurovascular bundle (Figs 8 and 10). The more extensive attachment of the MHGM toward the midline at the level of the intercondylar notch in the occluder group is likely to be the result of changes that occur during embryological migration of the MHGM across the popliteal fossa from lateral to medial. In the occluder group, it is possible that the more extensive position and attachment of the MHGM compresses and occludes the adjacent popliteal vasculature during contraction. Muscle hypertrophy in athletes may exacerbate the degree of arterial compression in those with greater midline MHGM attachment.

The clinical syndrome of entrapment and clinical implications. It is widely accepted that injury (biologic in atherosclerosis and mechanical in entrapment) and the associated inflammatory response processes may lead to degeneration and arterial occlusion. In entrapment, the extent of degeneration depends on the magnitude of the force applied to the wall, consisting of the mass of the muscle, the accelerative forces it imposes, and how often this occurs within a specific time period. In the case of embryological or classical entrapment, neurovascular injury is caused by an abnormally placed muscle or fibrotendinous band.^{1,11,16,17} In athletes, hypertrophy and rapid movement of the anomalous muscle or band is likely to cause injury, leading to degeneration or aneurysm formation.^{13,14,18} Intense exercise may temporarily occlude the artery and induce symptoms such as calf or foot claudication, paresthesia, coldness, and numbness.^{15,18} Ankle pulses are normal at rest if degeneration and occlusion has not occurred.

Rarely, occlusion can lead to critical ischemia (rest pain and tissue loss).¹⁸ Because repetitive injury is likely to lead to degeneration, surgical treatment is recommended when classic entrapment is diagnosed.¹⁸ The offending muscle or fibrous band should be excised and the popliteal artery replaced with saphenous vein if degeneration has occurred. In symptomatic functional entrapment, the mechanism that leads to injury remains unclear.

Although the popliteal arteries in 30% to 50% of the normal population will be compressed on forceful MHGM contraction, few of these individuals appear to become symptomatic, and only a small number of these are likely to go on to arterial degeneration and occlusion.^{2,3,5,18} Athletes again seem to be at risk. Some reports suggest that symptoms in selected athletes may be due to nerve compression or a form of localized compartment syndrome.¹

Symptomatic individuals seem to benefit from surgery. This involves the releasing of various muscle attachments, which intraoperatively appear to be involved in the entrapment mechanism.^{1-3,5,18} The overall prognosis of functional entrapment appears to be better than embryological entrapment.

We and others have shown that under test conditions of forceful plantar flexion, local forces are sufficient enough in some individuals to cause arterial compression. Because the functional syndrome is rare, it is likely that muscle movement associated with daily activity and social exercises may not generate sufficient force to occlude and injure the artery in most occluders. Such a common entity in a general population cannot be ignored, and pertinent questions remain unanswered:

- What are the precise anatomic risk factors in the small group of young individuals who become symptomatic?
- Is there a potential for cumulative injury (biologic and mechanical) in older individuals with atherosclerotic risk factors?
- What is the best surgical option to treat symptomatic individuals?

Although we have not shown conclusively that the variation described leads to the clinical syndrome, this new information may form a platform for future studies. Hence, studying the attachment of the MHGM on young symptomatic functional occluders, in claudicant patients with isolated or predominant popliteal artery occlusive disease, and in individuals with idiopathic venous hypertension is likely to provide important information. If the variation described does indeed lead to symptomatic entrapment, then the treatment option of dismantling only the midline attachment fibres of the MHGM, within and above the intercondylar notch, needs to be investigated.

The current classification of entrapment lists functional entrapment as type VI (ie, normal anatomy) and is regarded as a somewhat separate entity to the five embryological anomalies.^{7,18} The variation we describe may have an embryological basis in that compared with type II, the position of the MHGM is not as extreme; that is, there was better embryological timing between MHGM migration and fusion of the popliteal artery remnants. This may warrant a modification of the existing classification.

CONCLUSION

We have shown that in normal adult occluders, the MHGM attachment sites extend toward the midline of the bone above the medial condyle and within the intercondylar notch. The ensuing muscle bulk that arises from these attachment sites lies close to the neurovascular bundle. This is likely caused by “embryological lagging behind” of some muscle fibers as the MHGM migrates from a lateral to medial position during limb bed rotation in the embryo.

Although this study demonstrates a variation of normal MHGM attachment that could account for functional compression of the popliteal artery, it does not explain why the clinical entity of functional popliteal entrapment is so

uncommon. It is likely that an extreme normal variant of MHGM attachment close to the midline of the femur and within the intercondylar fossa causes injury to the adjacent neurovascular bundle during contraction. Further MRI studies of the MHGM in asymptomatic and symptomatic functional occluders are warranted.

AUTHOR CONTRIBUTIONS

Conception and design: JP, LL

Analysis and interpretation: JP, MH, MV

Data collection: JP, MH, MC

Writing the article: JP, LL, GC, MC, MV

Critical revision of the article: JP, LL, GC, MC, NV

Final approval of the article: JP, LL, MH, GC, MC, NV

Statistical analysis: JP, GC, MC

Obtained funding: Not applicable

Overall responsibility: JP

REFERENCES

1. Turnipseed WD, Pozniak M. Popliteal entrapment as a result of neurovascular compression by the soleus and plantaris muscles. *J Vasc Surg* 1992;15:285-94.
2. Rignault DP, Paillet JL, Lunel F. The "functional" popliteal artery entrapment syndrome. *Int Angiol* 1985;4:341-3.
3. Erdoes LS, Devine JJ, Bernhard VM, Baker MR, Berman S, Hunter GC. Popliteal vascular compression in a normal population. *J Vasc Surg* 1994;20:978-86.
4. Love JW, Whelan TJ. Popliteal artery entrapment syndrome. *Am J Surg* 1965;109:620-4.
5. Darling RC, Buckley CJ, Abbot WM, Raines JK. Intermittent claudication in young athletes: popliteal artery entrapment syndrome. *J Trauma* 1974;14:543-52.
6. Rizzo RJ, Flinn WR, Yao JST, McCarthy WJ, Vogelzang RL, Pearce WH. Computed tomography for evaluation of arterial disease in the popliteal fossa. *J Vasc Surg* 1990;11:112-9.
7. Fujiwara H, Sugano T, Fujii N. Popliteal artery entrapment syndrome: accurate morphological diagnosis utilizing MRI. *J Cardiovasc Surg* 1992;33:160-2.
8. Di Marzo L, Cavallaro A, Sciacca V, Lepidi S, Marmorale A, Tamburelli A, et al. Diagnosis of popliteal artery entrapment syndrome: the role of duplex scanning. *J Vasc Surg* 1991;13:434-8.
9. Hoffman U, Vetter J, Rainoni L, Leu AJ, Bollinger A. Popliteal artery compression and force of active plantar flexion in young healthy volunteers. *J Vasc Surg* 1997;26:281-7.
10. Ruppert V, Verrel F, Geppert SN, Sadeghi-Azandaryani M, Burklein D, Steckmeier B. Results of perioperative measurements of ankle-brachial index in popliteal artery entrapment syndrome. *J Vasc Surg* 2004;39:758-62.
11. Levien JL, Veller MG. Popliteal artery entrapment syndrome: more common than previously recognized. *J Vasc Surg* 1999;30:587-98.
12. Stuart TPA. Note on a variation in the course of the popliteal artery. *J Anat* 1879;13:162.
13. Rich NM, Collins GJ, McDonald PT, Kozloff L, Clagett GP, Collins JT. Popliteal vascular entrapment. *Arch Surg* 1979;114:1377-84.
14. Colborn GL, Lumsden AB, Taylor BS, Skandalakis JE. The surgical anatomy of the popliteal artery. *Am Surg* 1994;60:238-46.
15. Gibson MHL, Mills JG, Johnson GE, Downs AR. Popliteal entrapment syndrome. *Ann Surg* 1977;185:341-8.
16. Insua JA, Young JR, Humphries AW. Popliteal artery entrapment syndrome. *Arch Surg* 1970;101:771-5.
17. Bouhoutos J, Daskalakis E. Muscular abnormalities affecting the popliteal vessels. *Br J Surg* 1981;68:501-6.
18. Levien L. Popliteal artery entrapment syndrome. *Seminars in Vascular Surgery* 2003;16:223-31.

Submitted Feb 10, 2008; accepted Jun 22, 2008.